Published in final edited form as:
Biochim Biophys Acta. 2008 April ; 1780(4): 696–708. doi:10.1016/j.bbagen.2008.01.013.

BOTH THE N-TERMINAL FRAGMENT AND THE PROTEIN-PROTEIN INTERACTION DOMAIN (PDZ DOMAIN) ARE REQUIRED FOR THE PRO-APOPTOTIC ACTIVITY OF PRESENILIN-ASSOCIATED PROTEIN PSAP

Guozhang Mao, **Jianxin Tan**, **Yongchang Shi**, **Mei-Zhen Cui**, and **Xuemin Xu**[§]
From the Department of Pathobiology, College of Veterinary Medicine, The University of Tennessee, 2407 River Dr., Knoxville, TN 37996

Abstract

Presenilin-associated protein (PSAP) was originally identified as a PS1-associated, PDZ domain protein. In a subsequent study, PSAP was found to be a mitochondrial apoptotic molecule. In this study, we cloned the PSAP gene and found that it is composed of 12 exons and localizes on chromosome 6. To better understand the structure and function of PSAP, we have generated a series of antibodies that recognize different regions of PSAP. Using these antibodies, we found that PSAP is expressed in four isoforms as a result of differential splicing of exon 8 in addition to the use of either the first or the second ATG codon as the start condon. We also found that all these isoforms are localized in the mitochondria and are pro-apoptotic. Furthermore, our data revealed that the PDZ domain and N-terminal fragment are required for the pro-apoptotic activity of PSAP.

1. Introduction

Apoptosis, one of the mechanisms of cell death, has been implicated in the neurodegeneration observed in Alzheimer's disease (AD)[1] and other neurodegenerative disorders [1–7]. This apoptotic cell death has been reported to be affected by presenilins (presenilin-1 [PS1] and PS2. The involvement of presenilin in apoptosis was first suggested by a study showing that ALG-3, a mouse homolog of the C-terminal fragment of PS2, rescues a T-cell hybridoma from Fas-induced apoptosis [8]. Interestingly, as in the case of PS2, the C-terminal fragment of PS1 was also found to inhibit Fas-induced apoptosis in Jurkat cells [9]. In an effort to understand the apoptotic regulatory effect of the C-terminal of PS1, we have identified a novel presenilin-associated protein (PSAP), which interacts with the C-terminal of PS1 [10]. Interestingly, in a subsequent study we found that PSAP is a pro-apoptotic protein that causes apoptosis when it is overexpressed [11]. This finding provides a direct molecular link between presenilin and the apoptotic pathway and also places PSAP in an important position in apoptosis.

[§]To whom correspondence should be addressed. Tel. 865-974-8206; Fax 865-974-5616; E-mail: xmx@utk.edu.

[1]The abbreviations used are: AD, Alzheimer's disease; PS, presenilin; PSAP, presenilin-associated protein; siRNA, small interfering RNA; FISH, fluorescence in situ hybridization; SMART, Simple Modular Architecture Research Tool.

Two major pathways lead to apoptotic cell death: namely, the cell surface death receptor-mediated pathway and the mitochondria-mediated pathway [12]. In the death receptor-mediated pathway, extracellular stimuli activate apoptotic cascades via binding and activation of cell surface death receptors. On the other hand, in the mitochondria-mediated pathway, apoptotic cascades are activated by small molecules, such as cytochrome c and apoptosis-inducing factor (AIF), released from the mitochondrial intermembrane space into the cytoplasm. In this regard, it is notable that PSAP is localized in mitochondria and that overexpression of PSAP causes release of cytochrome c from mitochondria [11], suggesting that PSAP causes apoptosis through a mitochondria-mediated pathway.

Since the report of the identification of PSAP, several groups have reported the cDNAs for PSAP from different species by directly depositing the DNA sequence information into the GenBank. Now the PSAP gene is also known as mitochondrial carrier homolog 1 (Mtch1). These DNA sequences revealed an important fact that some of the reported cDNAs are missing 51 nucleotides in the 3′-half of the coding region, suggesting the presence of different splicing isoforms of mRNA for PSAP. This information prompted us to determine the structures of the gene and protein of PSAP and their relationship with the biological function of PSAP. In the current work, we report that PSAP is expressed in two isoforms as a result of alternative splicing and that both isoforms are apoptotic active. We sought to discover whether these potential isoforms are indeed expressed under physiological conditions and whether these isoforms may have different biological functions. In addition, we sought to determine the relationship between the structure and function of PSAP.

2. Materials and methods

2.1. Cell culture and transfection

HEK293 cells were cultured in Dulbecco's modified Eagle's medium (DMEM) supplemented with 10% fetal bovine serum, 50 units/ml penicillin, and 50 μg/ml streptomycin. Transfection was performed using LipofectAMINE 2000 transfection reagent (Invitrogen). PSAP-myc fusion protein expression plasmid was constructed as described previously [11]. All deletion and truncation mutants were constructed using the site-directed mutagenesis kit (Stratagene).

2.2. Mitochondria isolation and proteinase treatment

Mitochondria were isolated as described previously [11]. Briefly, HEK 293 cells were harvested and washed with phosphate buffered saline once and swelled with 10 volumes of Swell buffer A (20 mM Hepes, pH7.9, 1.5mM NaCl, 10mM KCl, 0.5 mM β-mercaptoethanol) for 5 min on ice. After 500×g centrifugation at 4°C for 5 min, the cells were resuspended in 10 volumes of Swell buffer A and ruptured with 5 or 6 strokes with a Dounce Homogenizer using a tight-fitting pestle (pestle B). Sucrose (166.35μl, 60%) was added into each 1 ml of ruptured cells to reach a final concentration of 250 mM (iso-osmolar solution). After centrifugation at 800×g for 10 min at 4°C to remove the unbroken cells and nuclei, the supernate was layered on top of the sucrose gradients consisting of 30%, 35%, 40%, 43%, 46%, 50%, 55% and 60% sucrose, each in 4ml of 10 mM Tris-HCl, pH 7.4, 1 mM EDTA. The mixture was centrifuged at 60,000 × g in a Beckman SW 28.1 Rotor for 45 min at 4°C. Ten fractions or layers were collected using a 20-gauge needle, and the mitochondria-containing fractions were determined by Western blotting for the presence of cytochrome c. The intact mitochondria were collected from layers 3 and 4 (damaged or ruptured mitochondria go to the lower layer). After dilution with 3 volumes of distilled water, mitochondria were pelleted by centrifugation at 9,600 × g at 4°C for 15 min. The pellet was then resuspended in Buffer B (250 mM sucrose, 10 mM Tris-HCl, pH 7.4). The integrity of mitochondria was determined by measuring the activity of citrate synthase in the

presence and absence of 1% Triton X-100 (w/v), following the method of Robinson et al [13]. The presence of 1% Triton X-100 (w/v) has been shown to completely damage mitochondria [13, 14]. After confirming their integrity, the intact mitochondria were treated with trypsin (20 μg/ml, at 37 °C), chymotrypsin (25 μg/ml, at 37 °C), and proteinase K (5 μg/ml, at 4 °C) in a time course. The ruptured mitochondria were prepared by passing the isolated mitochondria in solution B through a 22-gauge hypodermic needle 120 times; the complete rupture of mitochondria was confirmed by measuring the activity of citrate synthase.

2.3. Immunoprecipitation and Western blotting

For routine Western blot analysis, cells or purified mitochondria were lysed by sonication for 20 s on ice in Western blot lysis buffer (50 mM Tris-HCl, pH 6.8, 8 M urea, 5% β-mercaptoethanol, 2% SDS, and protease inhibitor mixture from Roche Applied Science). The brain tissues from humans and other animals were first homogenized in Western blot lysis buffer using a Lab homogenizer (Polyton Kinematica, Switzerland) before sonication. After adding 4× SDS sample buffer and incubating at 65 °C for 15 min, samples were subjected to SDS-PAGE (8% for PARP and full length PSAP, 10–14% for truncated PSAP mutants, 10–16% for cytochrome *c*) and transferred to a polyvinylidene fluoride membrane (Immobilon-P, Millipore). The membranes were probed with appropriate antibodies (monoclonal antibodies against epitope myc (Santa Cruz), PARP (7D3-6, BD PharMingen), and cytochrome *c* (PharMingen) and visualized by ECL-Plus (GE Healthcare Biosciences) as described previously [11].

For co-immunoprecipitation, cells were harvested and homogenized in buffer A (30 mM HEPES, pH 7.5, 10 mM KCl, protease inhibitor mixture) by passing through a 20-gauge needle 30 times. The homogenized samples were centrifuged at 800 × g for 10 min to remove the unbroken cells and nuclei. The post nuclear supernates were centrifuged at 20,000 × g for 1 h, and the resulting membrane pellets were resuspended in 1 ml IP buffer (1% CHAPSO, 30 mM Tris, pH 8.0, 150 mM NaCl, 5mM EDTA containing cocktail protease inhibitors) and sonicated for 10 s on ice at 80% power employing a Fisher Sonic Dismembrator Model 300 with a 3.5 mm diameter tip. The lysates were cleared by centrifuging at 14,000 × g for 5 min at 4°C, and the supernates were subjected to co-immunoprecipitation using appropriate antibodies, followed by Western blot analysis as described previously [11].

2.4. Immunofluorescence Microscopy

HEK293 cells were plated on poly-L-lysine-coated coverslips and grown in DMEM containing 10% fetal bovine serum. The wild type PSAP construct and its mutants were transfected into HEK293 cells on the second day. 12 hrs after transfection, the medium was replaced with fresh medium containing 100 nM MitoTracker Red (Invitrogen, Carlsbad, CA) and incubated for 30 min to label the mitochondria. Cells were fixed in pre-warmed 3.7% paraformaldehyde in PBS was employed to fix cells at 37°C for 20 min, followed by permeablization with 0.2% Triton X-100 for 4 min. The fixed and permeablized cells were washed four times with PBS and blocked with 1% bovine serum albumin and 5% normal goat serum in PBS. The coverslips were incubated overnight with a monoclonal anti-Myc antibody (1:130, Santa Cruz Biotechnology, Santa Cruz, CA.), and then rinsed four times with PBS. After incubation with green-fluorescent Alexa Fluor 488 dye conjugated to goat anti-mouse IgG (1:150, Invitrogen) for 1 hr, the coverslips were washed four times with PBS and mounted with Supermount mounting medium (BioGenex, San Ramon, CA). Coverslips were examined under a fluorescence microscope (Nikon Eclipse E600) equipped with a digital camera.

2.5. Genomic DNA isolation and fluorescence in situ hybridization (FISH)

To isolate the genomic DNA for PSAP, a human genomic DNA bacteriophage P1 library (Genome Systems, Inc., St. Louis, MO) was screened by PCR using a pair of primers designed on the cDNA sequence of PSAP (custom service provided by Genome Systems, Inc., St. Louis, MO). One of the two clones, which contain the full-length genomic DNA for PSAP, was used as a probe in a FISH analysis to determine the chromosomal localization of the PSAP gene (custom service provided by Genome Systems, Inc., St. Louis, MO). DNA was labeled with digoxigenin-dUTP by nick translation. The labeled probe was combined with sheared human DNA and hybridized to normal metaphase chromosomes derived from human phytohemagglutinin-stimulated peripheral blood lymphocytes in a solution containing 50% formamide, 10% dextran sulfate, and 2× SSC. Specific hybridization signals were detected by incubating the hybridized slides in fluoresceinated anti-digoxigenin antibodies followed by counterstaining with 4,6-diamidino-2-phenylindole.

2.6. RNA interference

A small interfering RNA (siRNA) duplex was generated by Qiagen, Inc. (Valencia, CA) against the mouse *PSAP* (CTGGGATTCTTCGTTGGCTTA), which corresponds to nucleotides 694–714 downstream from the first ATG codon of the human PSAP coding region (exon 7). A control siRNA duplex (AATTCTCCGAACGTGTCACGT) that does not target any sequence in the genome (by Blast search) was also purchased from Qiagen, Inc. siRNAs were transfected into neuroblastoma N2a cells with HiPerfect transfection reagent (Qiagen), following the instructions provided by Qiagen, on the first and third days. Cells were harvested at 48 hrs and 72 hrs after transfection, lysed in Western blot lysis buffer, and subjected to SDS-PAGE electrophoresis and Western blotting analysis with Ab1 and Ab3 antibodies. N2a cells were cultured and maintained in DMEM supplemented with 10% fetal bovine serum as described previously [15].

3. Results

PSAP gene is localized on chromosome 6

Using the Bacteriophage P1 system, which offers the ability to clone large genomic DNA fragments between 70–95 kb in size with efficiencies approaching those of cosmids [16], we have isolated the genomic DNA for PSAP from a P1 human genomic DNA library. Two clones, 198 and 375, which bear the PSAP gene, were isolated. One of the two clones, clone 198, which contains a 90 kb insert, was sequenced and found to contain the full-length genomic DNA for PSAP. Using this clone 198 as a probe, we performed a FISH analysis experiment to determine the chromosomal localization of the PSAP gene. This experiment resulted in the specific labeling of the short arm of chromosome 6. The specifically labeled chromosome 6 measurements demonstrated that the PSAP gene is located at a position that is 44% the distance from the centromere to the telomere of chromosome arm 6p, an area that corresponds to band 6p2l.3 (Fig. 1).

PSAP gene is composed of 12 exons

We carried out DNA sequence analysis of the P1 gene clone 198, and it was revealed that the PSAP gene is composed of 12 exons (Table 1 and Fig. 2). These observations were confirmed by the human genome DNA sequence information, which is available from NCBI (National Center for Biotechnology Information).

PSAP is expressed in two splicing isoforms in humans and other animals

DNA sequence analysis also revealed three ATG codons located in exon 1 and a TAA stop codon in exon 12, followed by a long 3′-untranslated region (Fig. 2). The second and third

ATG codons are 54 and 192 nucleotides from the first ATG codon, respectively. This raises a question as to which of these potential ATG start codons is indeed used under physiological conditions. In addition, a cDNA that lacks the last 51 nucleotides of exon 8 was also reported by direct submission of the cDNA sequence to NCBI (accession number AF176006), suggesting that the PSAP gene may be expressed in two isoforms. To determine the start codon, the possible different splicing isoforms, and the protein structure of the PSAP, we generated several polyclonal antibodies using peptides corresponding to different regions of PSAP. As shown in Fig. 2, Ab3 was raised by using a peptide corresponding to the first 15 amino acids encoded by the cDNA sequence between the first ATG and second ATG codons; Ab1 was raised by using a peptide corresponding to residues 21 to 35 of the N-terminus of PSAP371, which starts from the second ATG codon; Ab5 was raised using a peptide corresponding to amino acids 147 to 161 of $PSAP_{371}$; Ab2 was raised using a peptide of 14 amino acids corresponding to residues 270 to 283 of PSAP371; and a peptide corresponding to the last 15 amino acids of PSAP371 was used to raise Ab4. By employing these antibodies, the *in vivo* expression of PSAP in human brain tissues was analyzed. In order to determine whether these antibodies recognize the same protein, the sample was run in a single wide-well slab gel. After electrophoresis and being transferred to the polyvinylidene fluoride membrane, the membrane was sliced into five pieces and each piece was probed with a specific antibody. As shown in Fig. 3A, two bands were detected by Ab1 (lane 2), Ab3, Ab4 (lane 4), and Ab5 (lane 5) in the brain tissues. Interestingly, Ab2 (lane 1), which was raised against the peptide corresponding to residues encoded by the 51 nucleotides, a peptide that is missing in exon 8 of the putative splicing isoform, detected only the upper band ($PSAP_L$), but not the lower band ($PSAP_s$). This result clearly indicates that PSAP is indeed expressed in two isoforms, the long form $PSAP_L$ and the short form $PSAP_S$, both of which are apparently a result of alternative splicing within exon 8.

Next, we examined the expression of PSAP in other animals. As shown in Fig. 3B, in addition to their presence in human brain tissue, two similar isoforms of PSAP were detected in the brain tissues of mouse, dog, cow, and horse. These results indicate that the two isoforms of PSAP are well conserved among mammals.

PSAP is mainly expressed utilizing the second ATG codon

In addition, the fact that these two $PSAP_L$ and $PSAP_S$ isoforms were equally detected by Ab1, Ab3, Ab4, and Ab5, indicates that none of them was expressed from the third ATG codon, mainly because Ab1 is not capable of detecting any peptide expressed from the third ATG codon. However, it was noted that the bands detected by Ab3 (Fig. 3A, lane 3) migrate slower than the bands detected by other antibodies. To further confirm that the bands detected by Ab3 are different from the bands detected by Ab1, Ab4, and Ab5, a sample prepared from human brain tissue was run in a single wide-well slab gel. After electrophoresis and being transferred to the polyvinylidene fluoride membrane, the membrane was sliced into three pieces, and each piece was probed with a specific antibody. As shown in the left panel of Fig. 3C, the mobility of the two bands detected by Ab3 (lane 2) is slower than that of the two bands detected by Ab1 (lane 1). Interestingly, when the membrane was probed with a mixture of both Ab1 and Ab3, four bands were detected (lane 3). This result clearly indicates that the two bands detected by Ab3 are different from the two bands detected by Ab1. As shown in the right panel of Fig. 3C, a similar four bands were also detected in mouse brain tissue. The fact that these two unknown bands were detected by Ab3, which is raised against the first 15 amino acids encoded by a cDNA sequence between the first ATG and second ATG codons, raises a possibility that the two bands detected by Ab3 are the polypeptides ($PSAP_{LL}$ and $PSAP_{LS}$), which are synthesized by using the first ATG codon. However, there is a question as to why $PSAP_{LL}$ and $PSAP_{LS}$ could not be detected by four other antibodies raised against other regions of the same

peptides. In this regard, we noticed that the titer of Ab3 is eight times higher than the other four antibodies. Thus, one possibility is that the levels of $PSAP_{LL}$ and $PSAP_{LS}$ are too low to be detected by Ab1, Ab4, and Ab5 under normal Western blotting conditions. Therefore, we performed the following immunoprecipitation experiments. As shown in the left panel of Fig. 3D, when samples were immunoprecipitated with Ab1(lane 1), Ab3(lane 2), Ab4(lane 3), and Ab5(lane 4) and probed with Ab1, in addition to $PSAP_L$ and $PSAP_S$ detected in lane 1, lane 3, and lane 4, two fine bands that correspond to $PSAP_{LL}$ and $PSAP_{LS}$ (lane 2) were also detected by Ab1. These fine bands that correspond to $PSAP_{LL}$ were also detected by Ab2, and both $PSAP_{LL}$ and $PSAP_{LS}$ were detected by Ab4 and Ab5 as well (data not shown) in the sample enriched by immunoprecipitation using Ab3. To further confirm this finding, we next performed reversed immunoprecipitation. The brain sample was immunoprecipitated with Ab1 and separated by a single wide-well slab gel. After electrophoresis and being transferred to the polyvinylidene fluoride membrane, the membrane was sliced into three pieces, and each piece was probed with a specific antibody. As shown in the right panel of Fig. 3D, Ab1 detected mainly $PSAP_L$ and $PSAP_S$ (lane 5). When the membrane was probed with Ab3, two bands that correspond to $PSAP_{LL}$ and $PSAP_{LS}$ were detected (lane 6). Furthermore, when the membrane was probed with a mixture of both Ab1 and Ab3, four bands were detected (lane 7). Actually, $PSAP_{LL}$ can also be immunoprecipitated by Ab2, and both $PSAP_{LL}$ and $PSAP_{LS}$ can be immunoprecipitated by Ab4 and Ab5 as well (data not shown). In addition, when cultured cells, such as HEK293 and Hela cells (from human origin) and N2a mouse neuroblastoma cells were used, similar results were observed (data not shown, but see below). The fact that $PSAP_{LL}$ and $PSAP_{LS}$ can be immunoprecipitated by Ab1, Ab2, Ab4, and Ab5 suggests that $PSAP_{LL}$ and $PSAP_{LS}$ are synthesized from the same mRNA as $PSAP_L$ and $PSAP_S$. To further test this possibility, we performed an *RNA interference* experiment. As shown in Fig. 3E, the same siRNA, which is designed based on the mouse cDNA corresponding to the cDNA sequence of exon 7 of the human PSAP gene, inhibited the expression of all the four polypeptides ($PSAP_{LL}$, $PSAP_{LS}$, $PSAP_L$, and $PSAP_S$) in N2a cells. Taken together, these results clearly indicate that $PSAP_{LL}$ and $PSAP_{LS}$ are the polypeptides expressed using the first ATG codon as the start codon.

To determine whether the Ab3-reactive $PSAP_{LL}$ and $PSAP_{LS}$ are the unprocessed precursors of $PSAP_L$, and $PSAP_S$, we constructed a plasmid that expresses $PSAP_{LL}$ with a myc tag fused to its C-terminal. As shown in Fig. 3F, only one band with a migration rate slower than endogenous $PSAP_{LL}$ was detected by anti-myc (lane 1) and Ab3 (lane 3), indicating that the N-terminus of $PSAP_{LL}$ was not removed from the recombinant protein. In addition, we also observed that $PSAP_{LL}$–myc is localized in the mitochondria and causes apoptosis when it is overexpressed (data not shown).

The N-terminus of PSAP is cleaved by trypsin

Several programs were used to analyze the secondary structure of PSAP, and different numbers of transmembrane domains are predicted by different programs. For example, two transmembrane domains (amino acids 230–252 and 297–319) were predicted by analysis using the Simple Modular Architecture Research Tool (SMART) search algorithms (http://smart.embl-heidelberg.de [17]); three transmembrane domains (amino acids 66–88, 230–249, and 297–319) were predicted by HMMTOP [18, 19], using the PredictProtein server (http://www.predictprotein.org/newwebsite/meta/submit3.php [20]); and six domains with an α-helix structure (amino acids 62–90, 135–156, 173–206, 238–262, 288–318, and 334–366) were predicted using the MINNOU protein trans-membrane prediction server (http://polyview.cchmc.org [21]). To precisely determine the topology of PSAP, mitochondria in which PSAP is localized [11] were isolated from HEK293 cells and treated with trypsin as described in the “Materials and Methods.” As shown in Fig. 4, both $PSAP_L$ and $PSAP_S$ were

detected in the intact mitochondria (lane 1 through the four panels), indicating that the deletion of the 17 amino acids as a result of differential splicing of exon 8 has no effect on the mitochondrial localization of PSAP. However, when the mitochondria were treated with trypsin, the fact that both $PSAP_L$ and $PSAP_S$ completely lost their immunoreactivity to Ab1 (top panel), which was raised against a peptide consisting of N-terminal residues 21 to 35 of PSAP (Fig. 2), indicates that the N-terminus of PSAP is sensitive to trypsin treatment. This sensitivity suggests that the N-terminus is more likely exposed on the surface of mitochondria, i.e. it is oriented toward the cytoplasm. In contrast, Ab4, which recognizes the extreme C-terminus of PSAP (Fig. 2), detected two bands (labeled as L* and S* with estimated molecular weights of 38 and 29 kDa, respectively, third panel), indicating that the C-terminus of PSAP remained intact during trypsin-treatment. In addition, these two L* and S* bands were also detected by Ab5 (bottom panel of Fig. 4), which was raised using a peptide corresponding to amino acids 147 to 161 of PSAP, indicating that the sequence from residue 147 to the C-terminal end of PSAP was not cleaved by trypsin. Since Ab2 was raised using a peptide corresponding to residues 270 to 283 of PSAP and recognizes $PSAP_L$ only, L*, which is generated from $PSAP_L$ by trypsin, was detected by Ab2 (second panel). These results indicate that, in intact mitochondria, only the N-terminus of PSAP is damaged by trypsin-treatment.

Chymotrypsin damages both the N-terminus and C-terminus of PSAP and cleaves PSAP into a short N-terminal and a long C-terminal fragment

The results demonstrated in Fig. 4 suggest two possibilities: the first is that both $PSAP_L$ and $PSAP_S$ are single transmembrane proteins with the N-termini exposed on the surface of mitochondria. The second possibility is that the PSAP protein could contain multiple transmembrane domains as predicted by the programs mentioned above; however, the C-terminus and the cytosolic-oriented hydrophilic loops between transmembrane domains are insensitive to trypsin, which is a highly sequence-specific proteinase and hydrolyzes the peptide bonds on the carboxyl side of arginine (R) and lysine (K). To test these possibilities, the isolated mitochondria were digested with chymotrypsin, a proteinase that has broader sequence-specificity than that of trypsin and cleaves on the C-terminal side of mainly F, Y, W M, and also I, S, T, V, H, G and A. As shown in Fig. 5, the loss of immunoreactivity of PSAP to Ab1 upon treatment with chymotrypsin indicates that, similar to trypsin-treatment, treatment of intact mitochondria with chymotrypsin also resulted in the cleavage of the N-terminus of PSAP (top panel, lanes 1 to 5). When the same samples were probed with Ab2, the N-terminal-truncated 38 kDa band (L*) was also detected (second panel) as in the case of trypsin-treatment. However, in contrast with trypsin-treatment, in which the L* band remained unchanged up to 2 h incubation, the L* band gradually and time-dependently decreased with a concomitant appearance and increase in a band of 25 kDa (second panel, lanes 1 to 5). Note that because the Ab2 recognizes only L*, the possible corresponding short peptide generated from S* was not detected by Ab2. It is also notable that this 25 kDa band was not detected by Ab5. In parallel with the decrease in L* and S* bands, a similar time-dependent formation of a 13 kDa band was detected by Ab5 (bottom panel, lanes 1 to 5). This result suggests that the L* band (and the S* band) was further cleaved by chymotrypsin, resulting in the formation of a 25 kDa C-terminal fragment that is immunoreactive to Ab2, and a 13 kDa N-terminal fragment that is immunoreactive to Ab5. It was also noted that upon treatment with chymotrypsin, L* and S* were detected by Ab4 as very fine bands up to 1.5 h incubation (third panel, lanes 2 to 4), suggesting that during chymotrypsin-treatment, the C-terminus of PSAP is damaged at the extreme end without affecting the migration of these L* and S* bands. This damage of the extreme C-terminus of PSAP may also explain why the 25 KDa band, which was detected by Ab2 (second panel), was barely detected by Ab4 (third panel, lane 5). The data presented in Fig. 5 also demonstrate that when the mitochondria were ruptured (by passing through a 20-gauge

needle 100 times in Homogenization Buffer), the bands detected by Ab2 became much thinner (second panel, lanes 7 to 10), and almost no band could be detected by Ab4 and Ab5, indicating that all the epitopes, which immunoreact with the antibodies used, were damaged (compare lanes 7 to 10 with lane 6 in all panels).

Proteinase K destroys all epitopes except the one recognized by Ab5

The data presented in Fig. 5 demonstrate that PSAP can be at least cleaved into short (13 kDa) N-terminal and large (25 kDa) C-terminal fragments by chymotrypsin. The extreme C-terminal end of PSAP is damaged by treatment with chymotrypsin. These results suggest that, in addition to the N-terminus, the C-terminus and at lease a portion of the peptide between the Ab5 and Ab2 epitopes are exposed to the surface of mitochondria. To further investigate this issue, we next treated the mitochondria with proteinase K, which is a serine protease with broad specificity towards aliphatic, aromatic and other hydrophobic amino acids (A, E, F, I, L, T, V, W or Y). As shown in Fig. 6, upon treatment with proteinase K, the 25 kDa C-terminal fragment became undetectable, indicating that the epitope for Ab2 was destroyed. However, the 13 kDa N-terminal fragment was still detected by Ab5 (bottom panel). As discussed later, this is most likely because the epitope for Ab5 is embedded in the membrane and protected from being digested.

PSAP is more likely a six-transmembrane protein

The data presented in Fig. 6 demonstrate that proteinase K destroyed all the epitopes except for the one recognized by Ab5. This observation rules out the possibility of a three-transmembrane model as predicted by the HMMTOP program in the PredictProtein server [20], because in the three-transmembrane model, the N-terminus and the C-terminus of PSAP must face away from each other. The data presented in Fig. 4 and Fig. 5 also ruled out the two-transmembrane model as predicted by the SMART server (http://smart.embl-heidelberg.de) [17, 22], because this model cannot explain the fact that a 13 kDa N-terminal fragment and a 25 kDa C-terminal fragment were produced by chymotrypsin-treatment and the fact that the 13 kDa N-terminal fragment is still detectable after treatment with proteinase K. As shown in Fig. 7A, six domains with an α-helix structure (amino acids 62 to 90, 135 to 156, 173 to 206, 238 to 262, 288 to 318, and 334 to 366) were predicted using the MINNOU protein trans-membrane prediction server [21]. Based on this prediction and the data presented in Fig. 4, 5, and 6, a six-transmembrane model of PSAP is proposed as illustrated in Fig. 7B. According to this model, the epitopes for Ab1, Ab2, and Ab4 are all on the same side and exposed to the surface of mitochondria, which is in agreement with the fact that all these epitopes are destroyed by proteinase K-treatment. The peptide (amino acids 147 to 161) used to raise Ab5 is a portion of the second transmembrane domain of PSAP, and thus it is protected from being digested by proteinase K. This protection may account for the fact that the 13 kDa N-terminal fragment is still detectable after treatment with proteinase K. The other possibility is that the epitope for Ab5 is on the opposite side, facing away from the cytosol, for example in a four-transmembrane model by rearranging numbers 1, 2, and 3 putative transmembrane domains (Fig. 7B). However, in any case the four-transmembrane model fails to explain the fact that a 13 kDa N-terminal fragment and a 25 kDa C-terminal fragment were produced from L* upon treatment with chymotrypsin.

The PSAP isoform, which is missing 51 nucleotides in exon 8, is still apoptotic

We have reported that full-length $PSAP_L$ is a mitochondrial apoptotic protein [11]. The presence of different isoforms of PSAP prompted us to determine whether $PSAP_S$, which lacks the region of loop 4 between the fourth and fifth transmembrane domains (Fig. 7B), is still capable of inducing apoptosis. To do so, we constructed four expression plasmids that express $PSAP_L$-myc, which is the full-length PSAP of 371 amino acids tagged with myc at its C-terminal; $PSAP_S$-myc, which is a splicing isoform of PSAP constructed by deleting the

17 amino acids (267 to 283) encoded by the 51 nucleotides that are missing in $PSAP_S$; ΔTM4-myc, which is constructed by deleting the region encoding the fourth transmembrane domain, amino acids 233 to 252; and ΔE8-myc, which lacks all the exon 8 encoding amino acids 236 to 284. As shown in Fig. 8A, the cleavage of PARP and the formation of the 85-kDa fragment of PARP, which is a characteristic of apoptosis [23], indicate that the deletion of the 51 nucleotides in exon 8 has no effect on the apoptotic activity of PSAP (top panel, lane 3). Moreover, it was also observed that deletion of the fourth transmembrane domain, which is the N-terminal portion of the peptide encoded by exon 8 (lane 5), and complete deletion of exon 8 (lane 4) had no effect on the apoptotic activity of PSAP.

Deletion of the N-terminal fragment and deletion of the putative PDZ domain causes dramatic reduction of the pro-apoptotic activity of PSAP

To further determine the structural requirement of the apoptotic activity of PSAP, we generated eight more truncation and deletion mutants of PSAP. As shown in the top panel of Fig. 8B, deletion of the N-terminal 138 residues, which includes the first transmembrane domain (Fig. 7B), resulted in complete abolishment of the apoptotic activity of PSAP (ΔN138, lane 6, top panel of Fig. 8B). However, C-terminal truncated mutant NPDZ, in which the 67 C-terminal amino acids were deleted, showed strong apoptotic activity (NPDZ, lane 2). Nevertheless, the C-terminal truncated mutant ΔCPDZ, in which the C-terminal 67 residues as well as the putative PDZ domain were deleted, showed no apoptotic activity (lane 7). This finding prompted us to determine whether the PDZ domain is necessary for the pro-apoptotic activity of PSAP. Interestingly, deletion of the putative PDZ domain alone led to a drastic decrease in the apoptotic activity of PSAP (ΔPDZ, lane 5). These results indicate that the region of the putative PDZ domain is required for the pro-apoptotic activity of PSAP. Moreover, deletion of the second mitochondria carrier domain, which partially overlaps with the PDZ domain, also resulted in a significant reduction of the apoptotic activity of PSAP (ΔMCH, lane 4). Data presented in Fig. 8B also showed that neither the PDZ domain alone (lane 9), the 67 amino acid C-terminal fragment (CTF, lane 10), nor the CPDZ (lane 8), which contains both the PDZ domain and the CTF, caused any apoptosis. The loss of the apoptotic activity of PSAP caused by the deletion of PDZ and MCH domains is apparently not due the expression levels of these mutants. In comparison with wild type PSAP and the mutant NPDZ, mutants ΔPDZ and ΔMCH were both expressed at relatively high levels. In fact, as shown in the middle panel of Fig. 8B, full-length PSAP (lane 2) and, specifically, mutant NPDZ (lane 3) were expressed at very low levels. The fact that these two peptides were detected at low levels is possibly due to the impaired cell machinery and cell death caused by these two constructs that showed strong pro-apoptotic activity.

Truncation of the N-terminal 138 residues causes loose association of PSAP with mitochondria

Since wild type PSAP is a mitochondrial protein, we next investigated the effects of these mutations on the subcellular localization of PSAP. We first performed the immunofluorescence microscopy analysis. Since all PSAP constructs were expressed with a myc tag conjugated to their C-termini, the intracellular PSAP and its mutants were immunolabeled with an anti-myc antibody (Santa Cruz). As shown in Fig. 9A, the green fluorescence (PSAP) in cells transfected with wild type PSAP as well as its mutants was found as punctuate structures (first column), which superposed nearly perfectly with the mitochondrial marker when column 1 was merged with column 2. These results indicate that, as with wild type PSAP, the truncation and deletion mutant PSAP were also localized in the mitochondria. Next, we performed a subcellular fractionation experiment to further determine the effects of these mutations on the mitochondrial localization. Cell lysates were fractionated by sucrose gradient centrifugation, as described under “Materials and Methods,” and subjected to Western blot analysis using specific antibodies. As shown in

Fig. 8C, the mitochondrial marker cytochrome c was primarily detected in fraction 3 and fraction 4 (bottom panel) by using a cytochrome c-specific antibody (PharMingen). Using a myc-specific antibody, we found that all PSAP mutants that contain the N-terminal fragment were also mainly detected in fractions 3 and 4 (second to fifth panels). These results, along with the observation using immunofluorescence analysis, indicate that these truncations and deletions had no effect on the mitochondrial localization of PSAP. However, the N-terminal truncation mutant ΔN138 was detected in fractions 2 through 6, but mainly in fraction 6 (top panel), in which only trace amounts of cytochrome c and other PSAP mutants were detected. These results indicate that deletion of the N-terminal 138 amino acids caused a loose association of PSAP with mitochondria and, as a result, the N-terminal truncated mutant ΔN138 was partially dissociated from mitochondria during subcellular fractionation procedure. Thus, the loss of the pro-apoptotic activity of ΔN138 is possibly, at least partially, due to the impaired association of PSAP to mitochondria.

Both the PDZ domain and the N-terminal fragment are involved in the interaction of PSAP with PS1

Next, we examined the effect of these mutations on the interaction of PSAP with PS1. As shown in the bottom panel of Fig. 8B, all mutants except the mutant CTF (lane 10) co-immunoprecipitated with PS1. Specifically, it was also noted that a very high amount of the PDZ peptide was co-immunoprecipitated with PS1 (lane 9), suggesting a strong interaction of this peptide with PS1. It was also noted that the mutants that contain the N-terminal fragment but lack the PDZ domain, such as ΔPDZ (lane 5) and ΔCPDZ (lane 7), were also co-immunoprecipitated with PS1, indicating that the PDZ domain is not the only fragment interacting with PS1. The low levels of these mutants co-immunoprecipitated with PS1 may be due to the low expression levels of these peptides (second panel) or due to both the low expression level and the lack of the PDZ domain. Notably, the mutant NPDZ was expressed at a very low level, and this may account for the very low amount of NPDZ co-immunoprecipitated with PS1 (lane 3). Taken together, these results suggest that both the PDZ domain and the N-terminal fragment are involved in the interaction of PSAP with PS1.

4. Discussion

In previous studies, we reported that PSAP is a pro-apoptotic mitochondrial protein. In the present study, we cloned the genomic DNA of PSAP and determined that the PSAP gene is located in the short arm of chromosome 6 (6p2l.3). We also determined that the PSAP gene is composed of 12 exons. Since the first report of the cloning of PSAP, a short cDNA that lacks 51 nucleotides in the 3′-half of the coding region was submitted directly to NCBI by several groups. This cDNA information suggests that PSAP may be expressed in two isoforms. To determine this possibility, we generated an antibody that is specific against the peptide encoded by the 51 nucleotides, which are missing in the short cDNA. By using this antibody in combination with four other antibodies that recognize other regions of PSAP, our data clearly demonstrate that PSAP is indeed expressed as two isoforms. The two isoforms are apparently a result of alternative splicing within exon 8, following the GT/AG rule. The fact that the two isoforms are detected in tissues of different animals indicates that the alternative splicing of PSAP mRNA is well conserved among mammals. In addition, there are three potential start ATG codons in the putative open reading frame of PSAP. By using a series of specific antibodies, our data clearly revealed that the third ATG codon was not used for expression of PSAP. Our data also revealed that though the majority of PSAP proteins were detected as $PSAP_L$ and $PSAP_S$, which lack the epitope encoded by the cDNA sequence between the first and second ATG codons, $PSAP_{LL}$ and $PSAP_{LS}$, which contain the epitope encoded by the cDNA sequence between the first and second ATG codons, were also detected in tissues and in cultured cells. These results suggest two possibilities: one possibility is that $PSAP_L$ and $PSAP_S$ are produced from $PSAP_{LL}$ and $PSAP_{LS}$ by

posttranslational removal of the N-terminal sequence; the other possibility is that either the first or the second ATG codon can be used as the start codon to express $PSAP_{LL}$/$PSAP_{LS}$ and $PSAP_L$/$PSAP_S$, respectively. The latter is supported by the fact that no signal peptide was suggested at the N-terminal of PSAP by any of the programs mentioned above nor by the software available at http://www.bioinformatics.leeds.ac.uk/prot_analysis/Signal.html. In addition, we have constructed an expression plasmid that expresses myc-tagged PSAP ($PSAP_{LL}$-myc), and we found that the recombinant $PSAP_{LL}$-myc was not processed at the N-terminal (Fig. 3F). Taken together, our data suggest that $PSAP_{LL}$ and $PSAP_{LS}$ are expressed using the first ATG as the start codon and that the majority of PSAP proteins, $PSAP_L$ and PSAP are expressed using the second ATG codon as the start codon.

In a previous study [11], we reported that PSAP shares homologues with mitochondrial carriers and, therefore, PSAP is also known as mitochondrial carrier homolog 1 (Mtch1) in the NCBI database. Mitochondrial carriers are referred to as a family of proteins localized in the inner membrane of mitochondria and exhibit a tripartite sequence structure, i.e. they contain three tandem repeated homologous domains about 100 amino acids in length. Each of these domains contains two hydrophobic stretches, which are thought to span the membrane as α-helices, separated by hydrophilic regions [24]. To determine the topology of PSAP, we developed several antibodies that recognize different regions of PSAP. After using these antibodies, our data suggest that PSAP also contains six transmembrane domains, though PSAP may only contain two typical repeated homologous domains [11]. However, our data clearly demonstrate that PSAP is localized in the outer membrane of mitochondria rather than the inner membrane.

It was noted that alternative splicing of exon 8 results in the deletion of 17 amino acids of most of the hydrophilic region between number 4 and number 5 transmembrane domains of PSAP. This finding prompted us to determine whether this differential splicing results in any variation in the pro-apoptotic activity of PSAP. Strikingly, we found that deletion of these 17 amino acids did not lead to notable changes in the pro-apoptotic activity of PSAP. Furthermore, during the course of topological study, it was also found that the deletion of the 17 amino acids between number 4 and number 5 transmembrane domains in the short form $PSAP_S$ has no effect on the topological structure and the mitochondrial localization of PSAP. The fact that both the long form $PSAP_L$ and the short form $PSAP_S$ maintain the same topological structure and residence in mitochondria may also account for the observation that both $PSAP_L$ and $PSAP_S$ equally induce apoptosis when overexpressed. These results also suggest that this region, which is missing the short form $PSAP_S$, is not required for PSAP to transduce apoptotic signals downstream. However, it cannot be ruled out that this region may be important for interactions with upstream regulators.

To further determine the structural and functional relationship of PSAP, we designed a series of deletion and truncation mutants of PSAP and tested for their apoptotic activities and mitochondrial localization. Using these mutations, we found that deletion of the other half of exon 8, which encodes the fourth transmembrane domain, or even the entire exon 8 has no effect on the mitochondrial localization and the pro-apoptotic activity of PSAP. Next, when the two other mutants, the N-terminal truncation mutant (ΔN138) and the C-terminal truncation mutant (NPDZ) were tested, it was found that deletion of the C-terminal 67 residues has no effect on the mitochondrial localization and the pro-apoptotic activity of the mutant PSAP. In contrast, deletion of the N-terminal 138 amino acids resulted in the abolishment of the pro-apoptotic activity of PSAP. Deletion of the N-terminal fragment of 138 amino acids also resulted in a partial dissociation of PSAP from mitochondria as determined by subcellular fractionation using sucrose gradient centrifugation. These results suggest that the loss of the pro-apoptotic activity of the N-terminal truncated PSAP mutant may be due to the impaired mitochondrial association. Is the mitochondrial localization

sufficient for the pro-apoptotic activity of PSAP? In this regard, it is notable that PSAP was thought to contain a putative PDZ domain [10] and that this putative PDZ domain remains intact in mutant NPDZ. Thus, we created a ΔCPDZ mutant in which, in addition to the C-terminal 67 amino acids, the PDZ domain was also deleted, and it was found that the pro-apoptotic activity of PSAP was completely abolished, though this mutant was still localized in mitochondria. Furthermore, our data clearly demonstrated that deletion of the PDZ domain alone also caused a drastic decrease in the pro-apoptotic activity of PSAP without affecting the mitochondrial localization. Although it cannot be completely ruled out that the deletion of the N-terminal fragment or the PDZ domain may cause conformational and topological changes in PSAP, resulting in the loss of its apoptotic activity, these results as well strongly suggest that mitochondrial localization and the region of the putative PDZ domain are essential for the pro-apoptotic activity of PSAP.

PDZ domains are found in diverse membrane-associated proteins and play an important role in protein-protein interaction and their assembly into supramolecular complexes [25]. In addition to serving as scaffolds, there is also evidence that PDZ domains can regulate the function of their ligands [26]. We have examined the effects of these mutations on the interaction between PSAP and PS1, and it was found that deletion of the PDZ domain has no significant effect on the interaction between PSAP and PS1. These findings suggest that this domain in PSAP may also mediate the interaction of PSAP with another molecule involved in PSAP-induced apoptosis. However, whether such a molecule exists and what possible role it plays in PSAP-induced apoptosis is currently not known.

In summary, our results demonstrate that PSAP is expressed in four different isoforms as a result of partially differential splicing of exon 8 and the use of either the first or the second ATG codon as the start codon. Our data also demonstrate that the differential splicing isoforms of PSAP ($PSAP_L$ and $PSAP_S$) show no differences in topological structure and mitochondrial localization and are equally pro-apoptotic. Our data further demonstrate that the N-terminal fragment is required for the tight association of PSAP with mitochondria and that both mitochondrial localization and the putative PDZ domain are required for the pro-apoptotic activity of PSAP. These results suggest that PSAP is involved in mitochondria-mediated apoptosis through interaction with other molecule(s) via its putative PDZ domain.

Acknowledgments

We thank Ms. Misty R. Bailey, College of Veterinary Medicine, The University of Tennessee, for her critical reading of the manuscript. This work was supported by grants from National Institutes of Health (NS42314) and the Alzheimer's Association (IIRG) to X. Xu and by a grant from National Institutes of Health grants HL074341 and the American Heart Association (0355339B) (to M.-Z. Cui)

References

1. Cotman CW, Anderson AJ. A potential role for apoptosis in neurodegeneration and Alzheimer's disease. Mol Neurobiol. 1995; 10:19–45. [PubMed: 7598831]
2. Cotman CW, Su JH. Mechanisms of neuronal death in Alzheimer's disease. Brain Pathol. 1996; 6:493–506. [PubMed: 8944319]
3. Masliah E, Mallory M, Alford M, Tanaka S, Hansen LA. Caspase dependent DNA fragmentation might be associated with excitotoxicity in Alzheimer disease. J Neuropathol Exp Neurol. 1998; 57:1041–1052. [PubMed: 9825941]
4. Ferrer I, Blanco R, Cutillas B, Ambrosio S. Fas and Fas-L expression in Huntington's disease and Parkinson's disease. Neuropathol Appl Neurobiol. 2000; 26:424–433. [PubMed: 11054182]
5. Sathasivam S, Ince PG, Shaw PJ. Apoptosis in amyotrophic lateral sclerosis: a review of the evidence. Neuropathol Appl Neurobiol. 2001; 27:257–274. [PubMed: 11532157]

6. Su JH, Zhao M, Anderson AJ, Srinivasan A, Cotman CW. Activated caspase-3 expression in Alzheimer's and aged control brain: correlation with Alzheimer pathology. Brain Res. 2001; 898:350–357. [PubMed: 11306022]
7. Su JH, Anderson AJ, Cribbs DH, Tu C, Tong L, Kesslack P, Cotman CW. Fas and Fas ligand are associated with neuritic degeneration in the AD brain and participate in beta-amyloid-induced neuronal death. Neurobiol Dis. 2003; 12:182–193. [PubMed: 12742739]
8. Vito P, Lacana E, D'Adamio L. Interfering with apoptosis: Ca(2+)-binding protein ALG-2 and Alzheimer's disease gene ALG-3. Science. 1996; 271:521–525. [PubMed: 8560270]
9. Vezina J, Tschopp C, Andersen E, Muller K. Overexpression of a C-terminal fragment of presenilin 1 delays anti-Fas induced apoptosis in Jurkat cells. Neurosci Lett. 1999; 263:65–68. [PubMed: 10218912]
10. Xu X, Shi Y, Wu X, Gambetti P, Sui D, Cui MZ. Identification of a novel PSD-95/Dlg/ZO-1 (PDZ)-like protein interacting with the C terminus of presenilin-1. J Biol Chem. 1999; 274:32543–32546. [PubMed: 10551805]
11. Xu X, Shi YC, Gao W, Mao G, Zhao G, Agrawal S, Chisolm GM, Sui D, Cui MZ. The novel presenilin-1-associated protein is a proapoptotic mitochondrial protein. J Biol Chem. 2002; 277:48913–48922. [PubMed: 12377771]
12. Budihardjo I, Oliver H, Lutter M, Luo X, Wang X. Biochemical pathways of caspase activation during apoptosis. Annu Rev Cell Dev Biol. 1999; 15:269–290. [PubMed: 10611963]
13. Robinson, BLGJB.; Sumegi, B.; Srere, PA. An enzymatic approach to the study of the Krebs tricarbossilic acid cycle. In: Darley-Usmar, VM.; Rick-wood, D.; Wilson, MI., editors. Mitochondria: A Practical Approach. IRL Press; Oxford: 1987. p. 153-170.
14. Lanni A, Moreno M, Lombardi A, Goglia F. Biochemical and functional differences in rat liver mitochondrial subpopulations obtained at different gravitational forces. Int J Biochem Cell Biol. 1996; 28:337–343. [PubMed: 8920643]
15. Zhao G, Cui MZ, Mao G, Dong Y, Tan J, Sun L, Xu X. γ-Cleavage is dependent on ζcleavage during the proteolytic processing of amyloid precursor protein within its transmembrane domain. J Biol Chem. 2005; 280:37689–37697. [PubMed: 16157587]
16. Sternberg N. Bacteriophage P1 cloning system for the isolation, amplification, and recovery of DNA fragments as large as 100 kilobase pairs. Proc Natl Acad Sci U S A. 1990; 87:103–107. [PubMed: 2404272]
17. Letunic I, Goodstadt L, Dickens NJ, Doerks T, Schultz J, Mott R, Ciccarelli F, Copley RR, Ponting CP, Bork P. Recent improvements to the SMART domain-based sequence annotation resource. Nucl Acids Res. 2002; 30:242–244. [PubMed: 11752305]
18. Tusnady GE, Simon I. The HMMTOP transmembrane topology prediction server. Bioinformatics. 2001; 17:849–850. [PubMed: 11590105]
19. Tusnady GE, Simon I. Principles governing amino acid composition of integral membrane proteins: application to topology prediction. J Mol Biol. 1998; 283:489–506. [PubMed: 9769220]
20. Vullo A, Frasconi P. Disulfide connectivity prediction using recursive neural networks and evolutionary information. Bioinformatics. 2004; 20:653–659. [PubMed: 15033872]
21. Porollo AA, Adamczak R, Meller J. POLYVIEW: a flexible visualization tool for structural and functional annotations of proteins. Bioinformatics. 2004; 20:2460–2462. [PubMed: 15073023]
22. Schultz J, Milpetz F, Bork P, Ponting CP. SMART, a simple modular architecture research tool: Identification of signaling domains. PNAS. 1998; 95:5857–5864. [PubMed: 9600884]
23. Dubrez L, Savoy I, Hamman A, Solary E. Pivotal role of a DEVD-sensitive step in etoposide-induced and Fas- mediated apoptotic pathways. EMBO J. 1996; 15:5504–5512. [PubMed: 8896444]
24. Palmieri F. The mitochondrial transporter family (SLC25): physiological and pathological implications. Pflugers Arch. 2004; 447:689–709. [PubMed: 14598172]
25. Ponting CP, Phillips C, Davies KE, Blake DJ. PDZ domains: targeting signalling molecules to sub-membranous sites. Bioessays. 1997; 19:469–479. [PubMed: 9204764]
26. Hung AY, Sheng M. PDZ Domains: Structural Modules for Protein Complex Assembly. J Biol Chem. 2002; 277:5699–5702. [PubMed: 11741967]

27. Mount SM. A catalogue of splice junction sequences. Nucleic Acids Res. 1982; 10:459–472. [PubMed: 7063411]

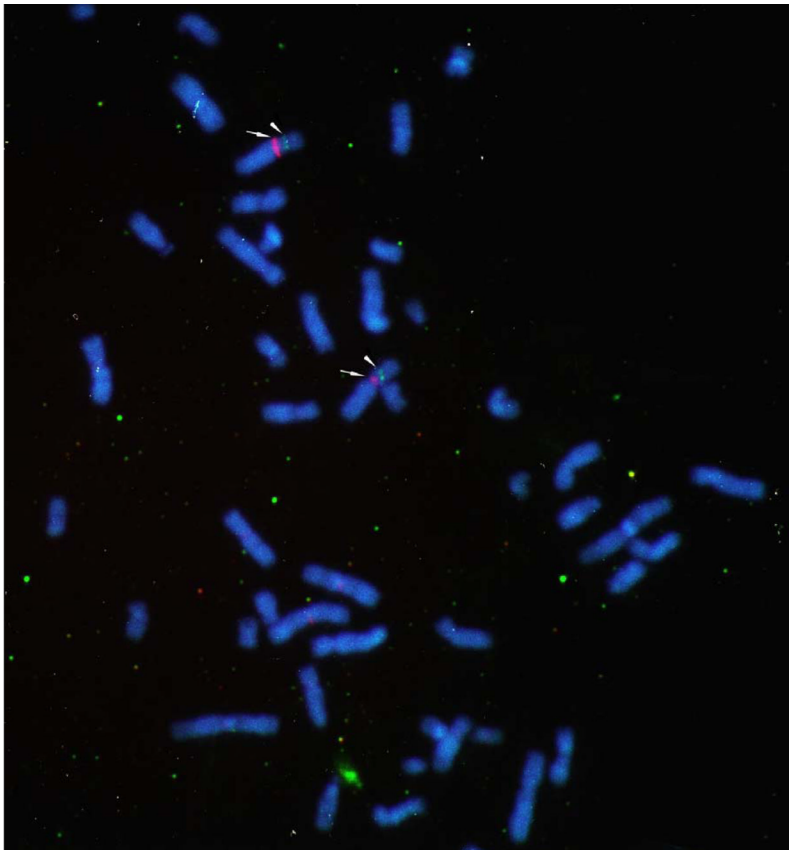

Figure 1. PSAP gene is localized on chromosome 6

The location of the PSAP gene was identified on chromosome 6p2l.3 by using a digoxigenin dUTP-labeled genomic DNA for PSAP (green, indicated by arrowheads). Co-localization on chromosome 6 was determined by co-hybridization with a biotinylated probe specific for the short arm of chromosome 6 (red, indicated by arrows).

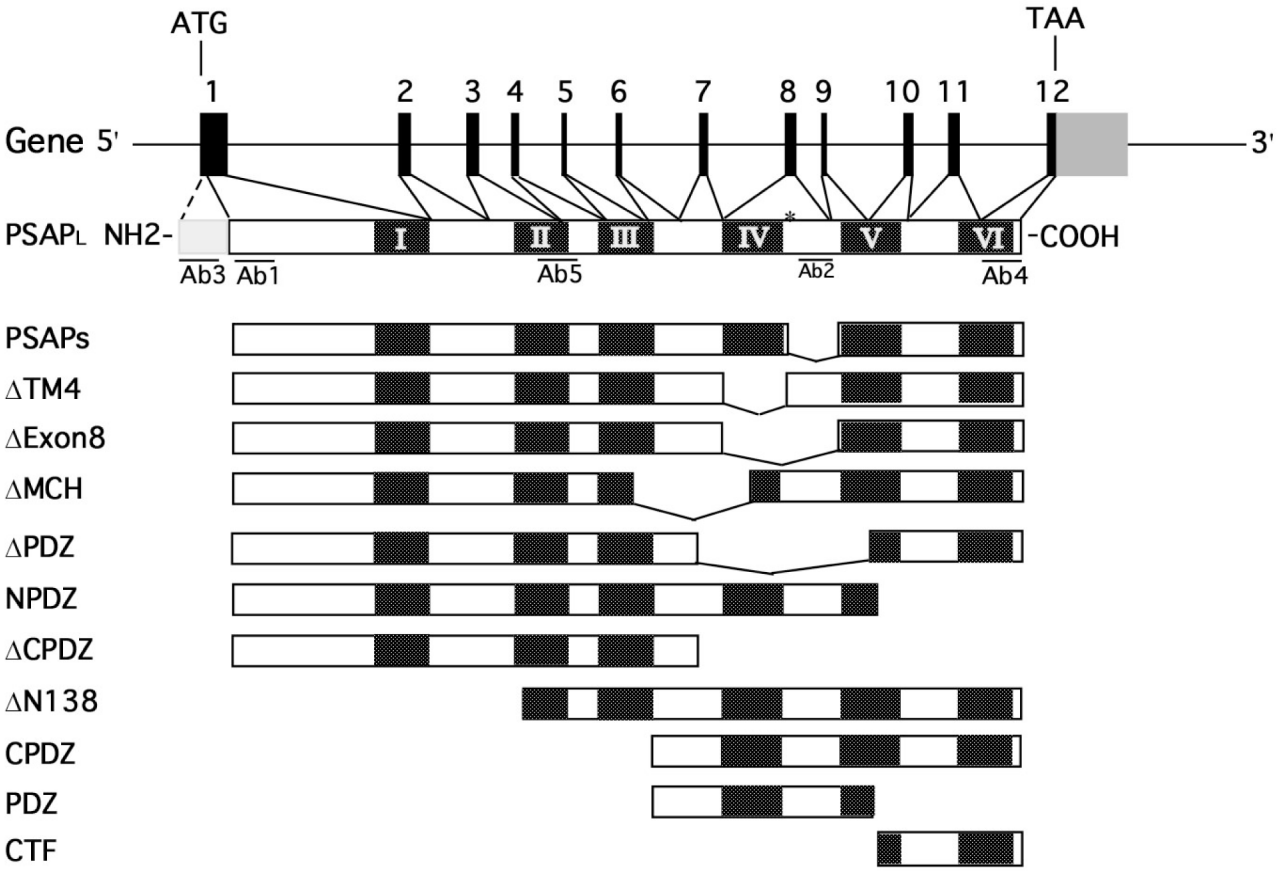

Figure 2. The gene structure and mutations of PSAP

Top, schematic presentation of PSAP gene exon/intron organization. Exons are indicated by vertical bars. Asterisk in exon 8 indicates the possible alternative splicing site. The untranslated region in exon 12 is shaded. Bottom, structure of the transcript product of $PSAP_L$, $PSAP_S$, and the engineered mutants. The predicted six transmembrane domains (I, II, III, IV, V, and VI) are indicated by dark-shaded boxes. Ab1, AB2, Ab3, Ab4, and Ab5 indicate the location of the epitopes recognized by these antibodies. The N-terminal light shaded box represents the epitope for Ab3, which is not expressed in PSAP.

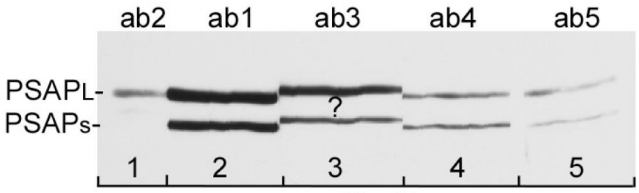

Fig. 3A

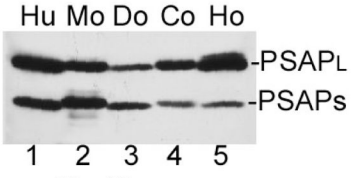

Fig. 3B

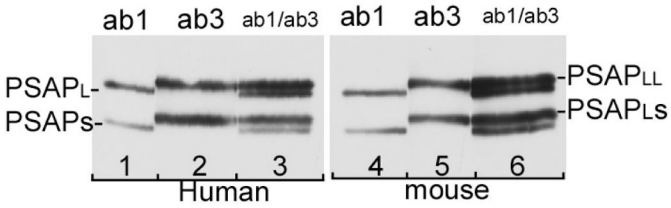

Fig. 3C

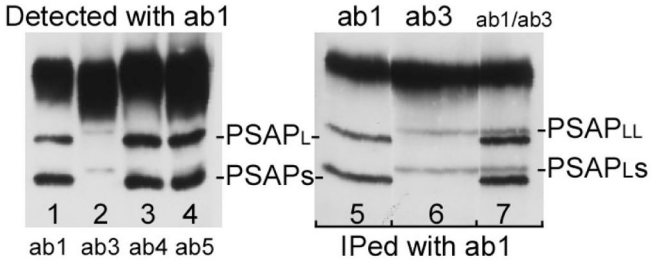

Fig. 3D

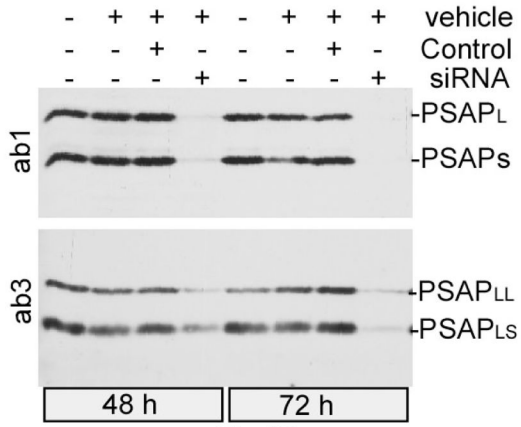

Fig. 3E

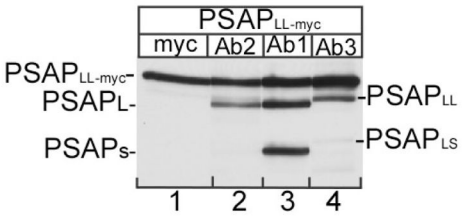

Fig. 3F

Figure 3. Identification of isoforms of PSAP

A , human brain tissues were analyzed by a single-wide-well slab gel (9%) electrophoresis and transferred to a membrane. The membrane was sliced into five pieces, and each piece was probed with a PSAP-specific antibody as indicated on the top of the panel. Ab1, Ab2, Ab4, and Ab5 were raised against different regions of PSAP; Ab3 was raised against a peptide of 15 amino acids encoded by the region between the first ATG and second ATG codons of PSAP cDNA. The question mark (?) in figure 3A indicates that the two bands detected by Ab3 are unknown. **B**, Western blot analysis of PSAP expression in brain tissues of human (Hu), mouse (Mo), dog (Do), cow (Co), and horse (Ho), using antibody Ab1. **C,** identification of $PSAP_{LL}$ and $PSAP_{LS}$. Human (left panel) and mouse (right panel) brain

tissues were analyzed by a two-wide-well slab gel (9%) electrophoresis and transferred to a membrane. The membrane was sliced into six pieces (three pieces for human brain sample and three pieces for mouse sample) and each piece was probed with a PSAP-specific antibody as indicated on the top of the panel. **D,** $PSAP_{LL}$ and $PSAP_{LS}$ were immunoprecipitated and detected by Ab1 and Ab3. Left panel, human brain sample was immunoprecipitated with Ab1 (lane 1), Ab3 (lane 2), Ab4 (lane 3), and Ab5 (lane 4) and probed with Ab1; right panel, the Ab1-immunoprecipitate complex was analyzed by a single-wide-well slab gel (9%) electrophoresis and transferred to a membrane. The membrane was then sliced into three pieces, and each piece was probed with a PSAP-specific antibody as indicated on the top of the panel. **E,** time course of knockdown of PSAP expression by small interfering RNA (**s**iRNA). Vehicle: transfection reagent; control: control RNA; siRNA: PSAP gene-specific small interfering RNA. After 72 hrs incubation, almost no $PSAP_L$ and $PSAP_S$ was detected by Ab1; however, small amounts of $PSAP_{LL}$ and $PSAP_{LS}$ were still detected, and this is possibly because of the high affinity of the Ab3 antibody, which can react with a low level of $PSAP_{LL}$ and $PSAP_{LS}$ and produce a strong signal. **F,** recombinant $PSAP_{LL}$ is not processed at its N-terminal. HEk293 cells were transfected with $PSAP_{LL}$-myc expression plasmid, and the cell lysate was analyzed by a single-wide-well slab gel (9%) electrophoresis and transferred to a membrane. The membrane was then sliced into four pieces, and each piece was probed with a PSAP-specific antibody as indicated on the top of the panel. Note that anti-myc antibody detects only the exogenous recombinant $PSAP_{LL}$-myc.

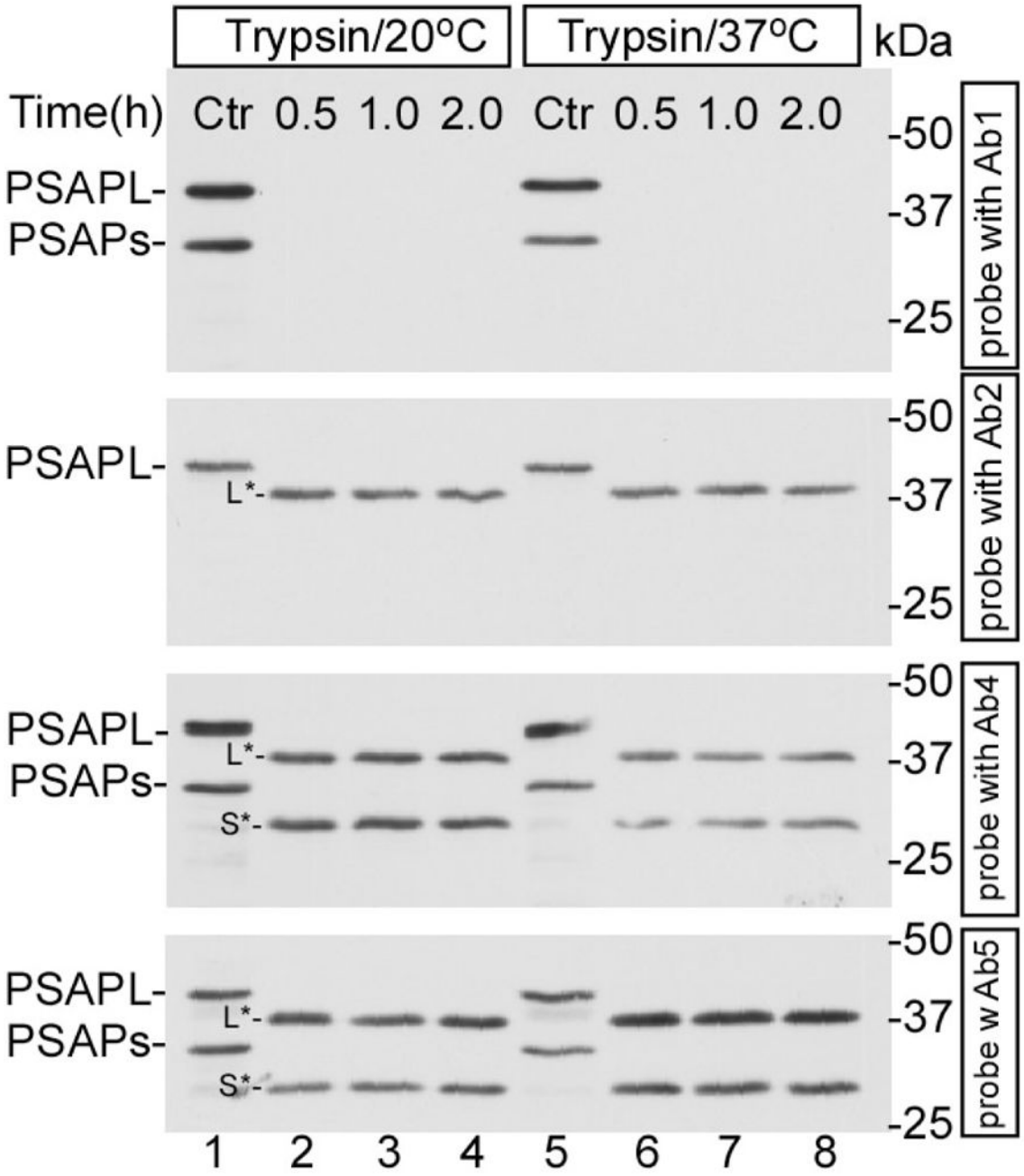

Figure 4. The N-terminus of PSAP is sensitive to trypsin digestion in intact mitochondria

Mitochondria were isolated from HEK293 cells and treated with trypsin at 20 °C (left) and 37 °C (right) in a time course. The reaction mixtures were analyzed by Western blotting using the four antibodies specific to different regions of PSAP. L* and S* are the trypsin-digested products from $PSAP_L$ and $PSAP_S$, respectively.

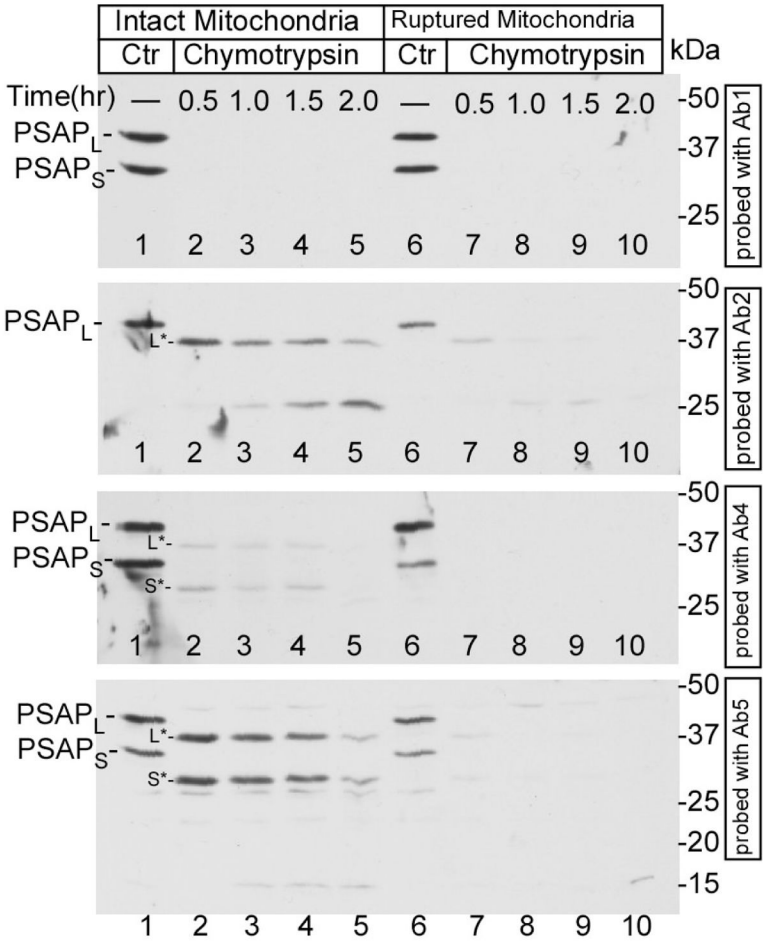

Figure 5. Chymotrypsin digestion of PSAP in intact and ruptured mitochondria

Left panel, mitochondria from HEK293 cells were treated with chymotrypsin at 37 °C in a time course. Right panel, mitochondria were ruptured and then treated with chymotrypsin as described under “Materials and Methods” at 37 °C. The reaction mixtures were analyzed by Western blotting using the four antibodies specific to different regions of PSAP. L* and S* are the N-terminal truncated peptides similar to the trypsin-digested products from $PSAP_L$ and $PSAP_S$, respectively. Notably, the L* and S* observed in chymotrypsin-digestion are similar to those observed in trypsin-digestion, but may not be exactly the same.

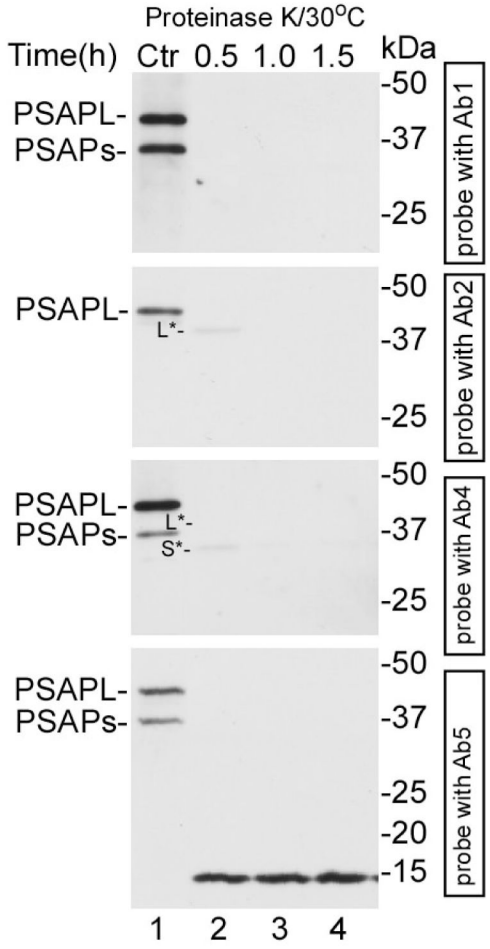

Figure 6. Proteinase K digestion of PSAP in intact mitochondria

Intact mitochondria from HEK293 cells were treated with proteinase K at 37 °C in a time course. The reaction mixtures were analyzed by Western blotting using the four antibodies specific to different regions of PSAP.

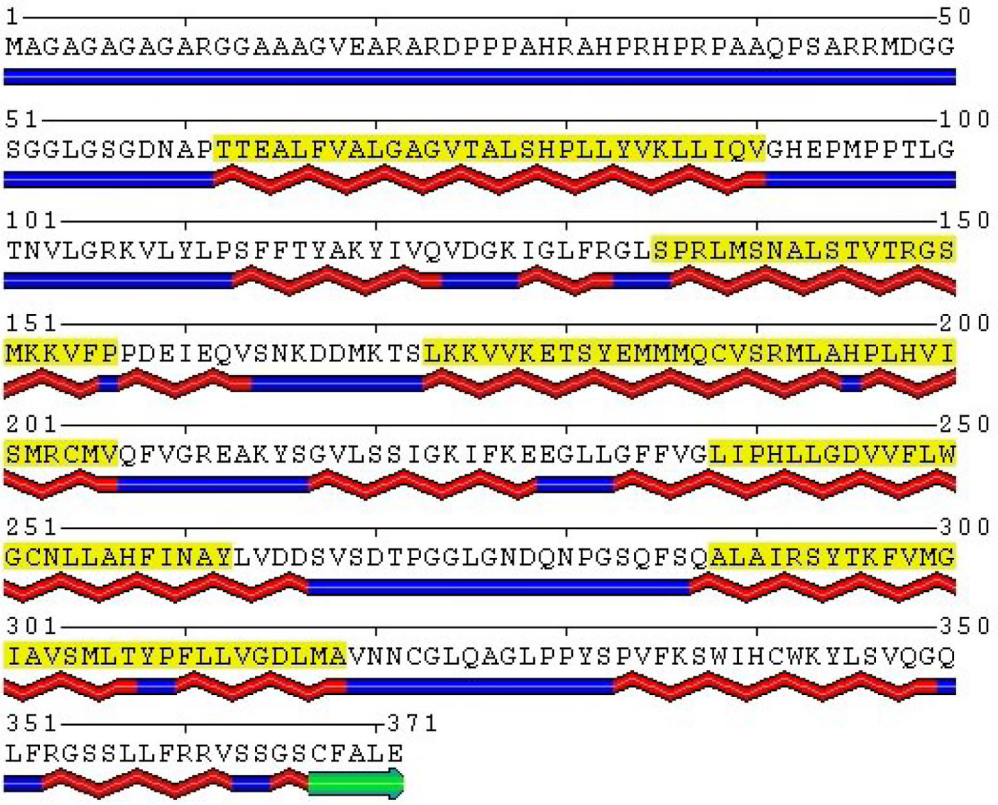

Fig. 7A

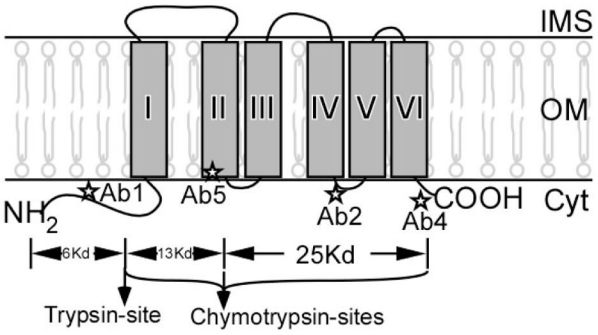

Fig. 7B

Figure 7. Predicted topological structure of PSAP

A six domains (red wavy lines) with an α-helix structure are predicted by the MINNOU protein trans-membrane prediction server [21]. The domains (amino acids 62–90, 135–156, 173–206, 238–262, 288–318) highlighted with yellow are predicted most likely to span the membrane. The last domain (amino acids 334–366) is also protected from being digested by trypsin and chymotrypsin. **B,** schematic illustration of the topological structure of PSAP. The epitopes for antibodies Ab1, Ab2, Ab4, and Ab5 are indicated by asterisks. The trypsin- and chymotrypsin-cleavage sites are indicated by vertical arrows.

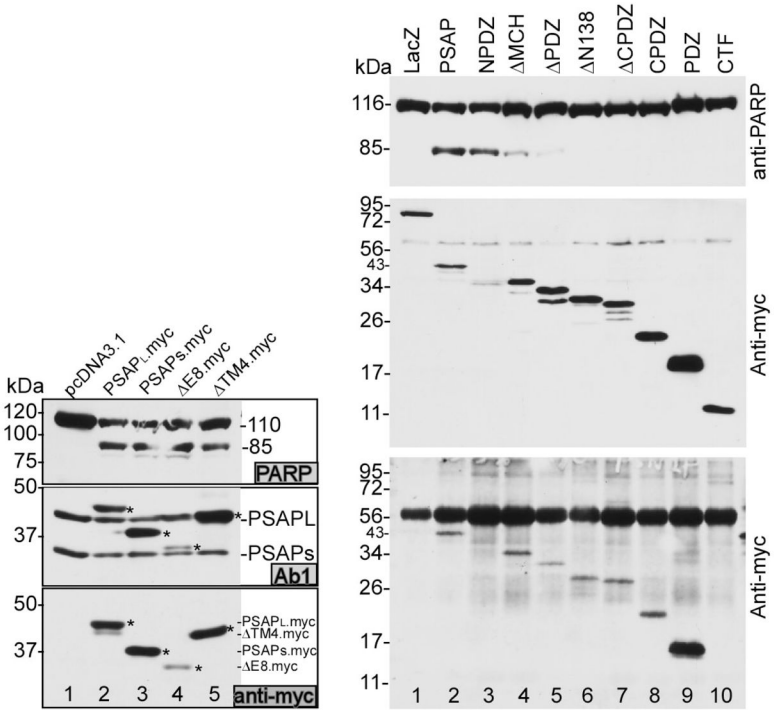

Figure 8. Pro-apoptotic activity of wild type and mutant PSAP

A, cell lysates from cells transfected with pcDNA3.1 vector (lane 1, mock transfected control), $PSAP_L$.myc (lane 2), $PSAP_S$.myc (lane 3), ΔE8.myc (lane 4), ΔTM4.myc (lane 5). Top panel probed with anti-PARP antibody; middle panel probed with PSAP-specific antibody Ab1, which interacts with both endogenous and exogenous PSAP; bottom panel probed with anti-myc antibody, which detects the myc-tagged exogenous protein only. * indicates the exogenously expressed PSAP and its mutants. Note that the myc-tagged mutant ΔTM4.myc migrates at a rate similar to that of endogenous $PSAP_L$. **B**, Through the three panels, lane 1 is the sample prepared from cells expressing myc-tagged Lac Z protein as a control. Lane 2 is the sample prepared from cells expressing wild type PSAP. Lanes 3 to 10 are samples prepared from mutant PSAP. Top panel are cell lysates probed with anti-PARP antibody to determine the pro-apoptotic activity of PSAP and its mutants. Middle panel are cell lysates probed with anti-myc antibody to determine the expression levels of PSAP and its mutants. Bottom panel are co-immunoprecipitation results. Cell lysates were immunoprecipitated with anti-PS1N, which recognizes the N-terminal fragment of PS1, and the immunoprecipitates were probed with anti-myc antibody as described in [11]. It is clear that Lac Z neither causes any apoptosis (top panel, lane 1) nor co-immunoprecipitates with PS1 (bottom panel, lane 1). In the second panel, the band detected at 60 kDa through all the samples (lanes 1 to 10) is a non-specific band. In the bottom panel, the band detected at 56 kDa through all of the samples (lanes 1 to 10) is the heavy chain of the rabbit IgG used for immunoprecipitation.

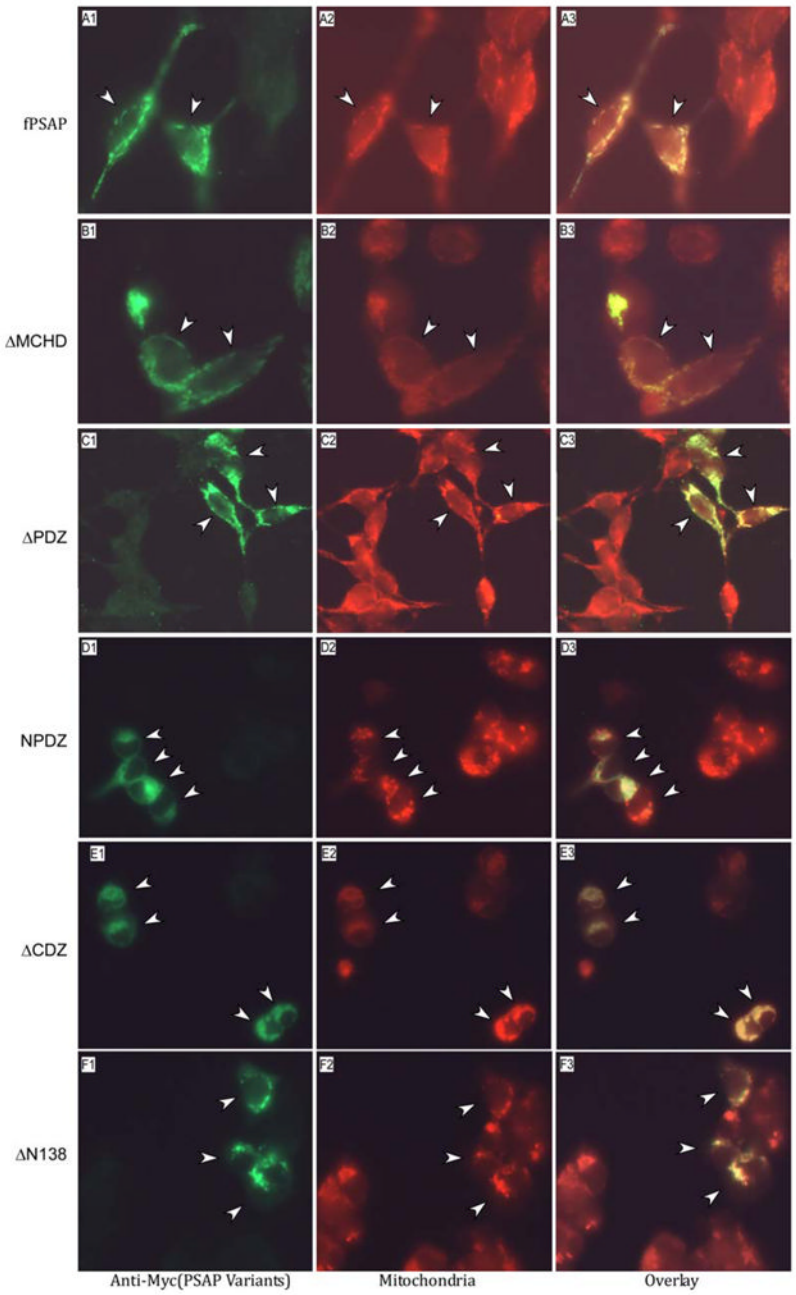

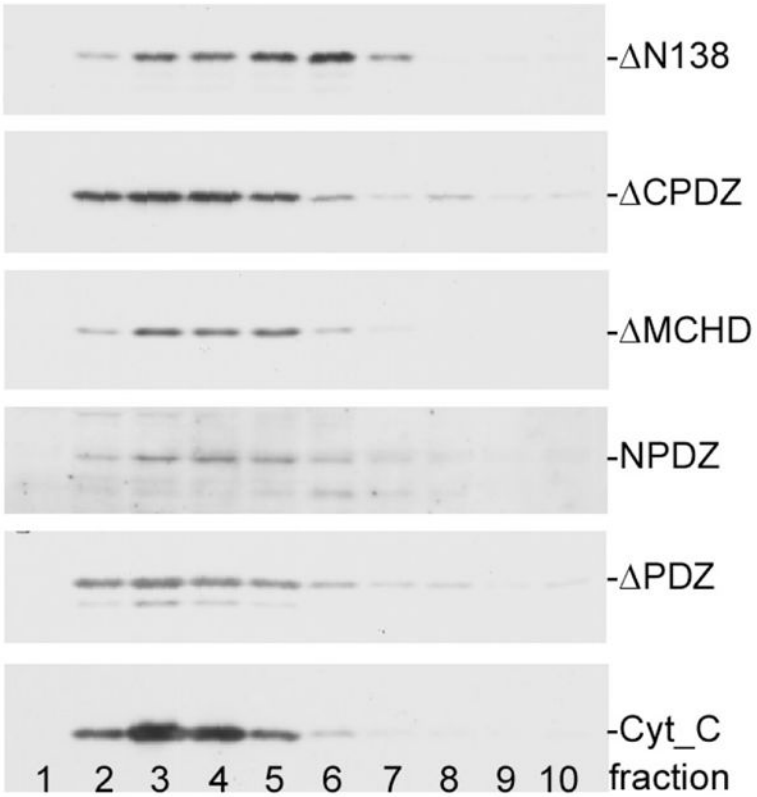

Figure 9. Mitochondrial localization of wild type and mutant PSAP

A Immunofluorescence microscopy analysis. In the first column (A1 to F1), the cells were stained for PSAP (green); in the second column (A2 to F2), the cells were stained for mitochondria (red); in the third column (A3 to F3), the images are the results of superimposing the images of column 1 on that column 2. Cells expressing PSAP or its mutants were indicated by arrowheads. **B.** Subcellular fractionation analysis. The bottom panel was probed with cytochrome c-specific antibody. The other panels were probed with anti-myc antibody to determine myc-tagged PSAP mutants.

Table 1

Intron/Exon boundaries of the human PSAP(MTCH1) gene

Exon number (size)	Intron number (size)	Sequence at intron/exon/intron junction
1 (321 bp)	1 (4183 bp)	ATG….TCCAGgtggg
2 (85 bp)	2 (2976 bp)	tgaagGTGGG….CTACGgtgag…
3 (107 bp)	3 (349 bp)	tacagCCAAG….AGAAGgtgag
4 (78 bp)	4 (386 bp)	ttcagGTTTT….AGGAGgtggg
5 (47 bp)	5 (397 bp)	tccagACCTC….GCCCAacccc
6 (52 bp)	6 (1492 bp)	caccaCCCCC….GGGAGccaag
7 (71 bp)	7 (2862 bp)	tcttcGCCAA….TTCGTgtacg
8 (145 bp)	8 (1957 bp)	tttagTGGAT….CCCAGgttgg
9 (48 bp)	9 (173 bp)	ctcagTTCAG….TGGGGgtaag
10 (68 bp)	10 (291 bp)	ttcagATTGC….TGCGGgtagg
11 (76 bp)	11 (1064 bp)	ggcagGCTGC….TGCAGgtgag
12 (72 bp)		tccagGGCCA….AGTAA3′UT

Introns are numbered at 3′ splicing acceptor, i.e. intron 1 precedes exon 2. The sequence of exons (uppercase letters) is flanked by introns (lowercase letters). The size of exon 1 was calculated from the first ATG codon, and the size of exon 12 was calculated up to the stop codon TAA. As shown, all the introns display splice signals consistent with the GT/AG rule [27], except intron 5 and 6. In intron 5, the 5′ splice donor is AC instead of GT, and the 3′ splice acceptor is CA instead of AG; in intron 6, the 3′ splice acceptor is TC instead of AG.